

# Azide vs Alkyne Functionalization in Pt(II) Complexes for Post-treatment Click Modification: Solid-State Structure, Fluorescent Labeling, and Cellular Fate

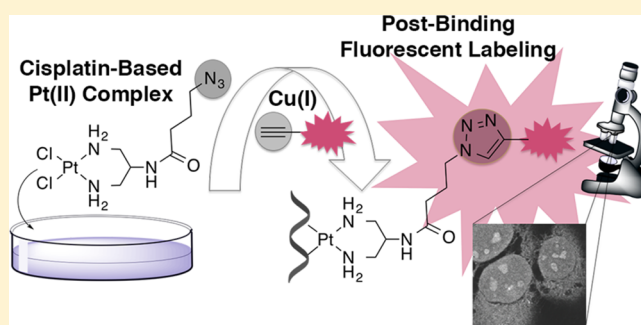
Regina Wirth,<sup>†</sup> Jonathan D. White,<sup>†</sup> Alan D. Moghaddam,<sup>†</sup> Aurora L. Ginzburg,<sup>†</sup> Lev N. Zakharov,<sup>‡</sup> Michael M. Haley,<sup>†</sup> and Victoria J. DeRose<sup>\*,†</sup>

<sup>†</sup>Department of Chemistry & Biochemistry and Institute of Molecular Biology, University of Oregon, Eugene, Oregon 97403-1253, United States

<sup>‡</sup>CAMCOR, University of Oregon, 1443 East 13th Avenue, Eugene, Oregon 97403, United States

## Supporting Information

**ABSTRACT:** Tracking of Pt(II) complexes is of crucial importance toward understanding Pt interactions with cellular biomolecules. Post-treatment fluorescent labeling of functionalized Pt(II)-based agents using the bioorthogonal Cu(I)-catalyzed azide–alkyne cycloaddition (CuAAC) reaction has recently been reported as a promising approach. Here we describe an azide-functionalized Pt(II) complex, *cis*-[Pt(2-azidobutyl)amido-1,3-propanediamine]Cl<sub>2</sub> (**1**), containing the *cis* geometry and difunctional reactivity of cisplatin, and present a comparative study with its previously described alkyne-functionalized congener. Single-crystal X-ray diffraction reveals a dramatic change in the solid-state arrangement with exchange of the alkyne for an azide moiety wherein **1** is dominated by a pseudo-chain of Pt–Pt dimers and antiparallel alignment of the azide substituents, in comparison with a circular arrangement supported by CH/ $\pi$ (C $\equiv$ C) interactions in the alkyne version. *In vitro* studies indicate similar DNA binding and click reactivity of both congeners observed by fluorescent labeling. Interestingly, complex **1** shows *in vitro* enhanced click reactivity in comparison to a previously reported azide-appended Pt(II) complex. Despite their similar behavior *in vitro*, preliminary *in cellulo* HeLa studies indicate a superior imaging potential of azide-functionalized **1**. Post-treatment fluorescent labeling of **1** observed by confocal fluorescence microscopy shows nuclear and intense nucleolar localization. These results demonstrate the potential of **1** in different cell line localization studies and for future isolation and purification of Pt-bound targets.



## INTRODUCTION

Since the compound cisplatin, *cis*-diamminedichloroplatinum(II), was approved by the FDA for clinical use in 1978, Pt-based therapeutics have become one of the most widely used and successful treatment options for a variety of cancers, including ovarian, testicular, bladder, non-small-cell lung carcinomas, and others.<sup>1–4</sup> Although much progress has been made in understanding the mechanisms of action of Pt compounds as well as their specific cellular targets, a comprehensive molecular-level understanding of their reactivity is still lacking.<sup>5–8</sup> It is generally accepted that Pt reagents are taken up into the cell via passive and active mechanisms and then undergo aquation, the displacement of labile chloride ligands by water, forming [Pt(NH<sub>3</sub>)<sub>2</sub>Cl(OH<sub>2</sub>)]<sup>+</sup> and [Pt(NH<sub>3</sub>)<sub>3</sub>(OH<sub>2</sub>)<sub>2</sub>]<sup>2+</sup> species.<sup>9,10</sup> These highly reactive species form exchange-inert complexes with purine bases of genomic DNA in addition to other biomolecules.<sup>11</sup> *In vivo* and *in vitro* studies have unambiguously identified *cis*-1,2-{Pt(NH<sub>3</sub>)<sub>2</sub>}<sup>2+</sup>-d(GpG), 1,2-d(ApG), and 1,3-d(GpNpG) intra- and interstrand DNA cross-links as products, and these are capable of inhibiting normal

transcriptional processes of the cell and initiating apoptotic signaling.<sup>12,13</sup> Importantly, only a very small fraction of Pt (less than 10% in the case of cisplatin) accumulates within genomic DNA.<sup>14</sup> In samples isolated from cells treated with Pt reagents, Pt has been found to bind to a wide variety of additional nucleophilic targets, including different cellular RNAs, proteins, and sulfur-containing compounds such as glutathione. Despite a great deal of work, Pt localization in treated cells and binding properties with non-DNA targets, and their consequences, remain poorly understood.<sup>6,7,15</sup> A better understanding of Pt cellular reactivity is essential in order to design new, more effective therapeutics and methods of delivery.

In addition to identifying molecular targets of Pt reagents, a comprehensive identification of all organelle targets is desired. Such an understanding would shed light on apoptotic and toxicity pathways, as well as differences in efficacy in dissimilar types of cancers. Highlighting the diversity of potential cellular

Received: August 31, 2015

Published: October 29, 2015

locales, various studies using atom-based techniques as well as fluorescent tagging have obtained evidence for cellular Pt accumulation in ribosomes, the nucleus, nucleoli, mitochondria, and secretory pathways linked to vesicles, lysosomes, and Golgi.<sup>16–18</sup>

Fluorescence detection via confocal microscopy has distinct advantages of sensitivity and resolution and can be coupled with existing fluorescent markers for co-localization studies. An important strategy used to detect Pt in cells comprises the covalent tethering of fluorescent probes to modified Pt-coordinated ligands. In one such study, a fluorescein-linked Pt compound was observed to accumulate in the nucleus and nucleolus 2–3 h post-treatment, followed by punctate localization in the cytoplasm after 7 h. A gradual decrease in total cellular fluorescence was observed over several days, indicating that Pt actively effluxes from the cells.<sup>17</sup> Other Pt–fluorescein conjugates have revealed accumulation in the Golgi and in vesicles, and expression of Cu efflux proteins was demonstrated to affect Pt retention.<sup>18</sup> Other important conclusions regarding the reactivity of Pt compounds have been determined via modification with fluorescent probes, and these have been reviewed recently.<sup>19</sup> While fluorophore-linked Pt probes have been shown to mimic some properties of native Pt complexes, the physical properties of the large, hydrophobic probes and their interactions within the cell are expected to be quite different from those of the small, neutral or positively charged Pt complexes.<sup>8,17–20</sup> These differences may influence the types of interactions that direct localization of the Pt complex, such as intercalation, hydrophobic, or electrostatic-based interactions. It has been shown, for example, that different amino-acid-linked cisplatin analogues exhibit altered specificity for ribosomal RNA (rRNA) compared to the parent compound.<sup>21</sup>

Due to possible undesirable consequences of pre-attaching probes, fluorescence detection of Pt compounds through post-binding modifications would be more attractive. This strategy takes advantage of minimally invasive reactive handles incorporated onto Pt reagents, followed by conjugation to fluorescent probes after the Pt compound has bound irreversibly to biomolecule targets (Figure 1). Using this strategy, we have previously reported use of the Cu-catalyzed azide–alkyne cycloaddition (CuAAC) click reaction,<sup>22</sup> with

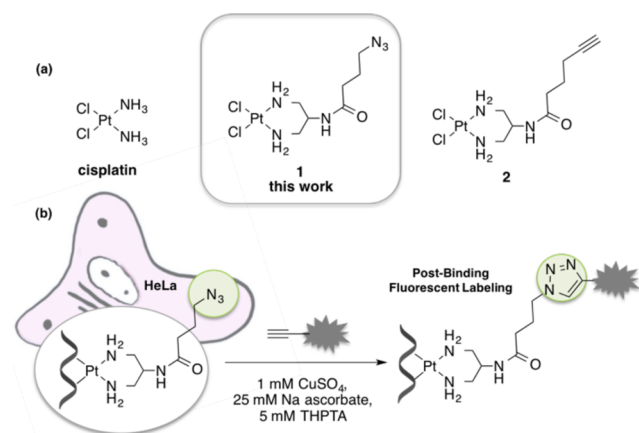


**Figure 1.** (a) Chemical structures of the anticancer drug cisplatin, with the novel azide-terminated 1 and alkyne-terminated 2. (b) Reaction scheme of target-bound 1 undergoing post-binding covalent click modification to a fluorescent probe.

modified Pt(II) complexes containing azide- and alkyne-reactive “handles”.<sup>23–26</sup> We have identified cellular RNAs, including tRNA, as targets of Pt reagents *in vivo*, in addition to identifying other nucleotide and protein targets *in vitro*.<sup>23–27</sup> Recently, Bierbach and colleagues have used post-binding click modification of a monofunctional Pt–acridine hybrid complex to identify its cellular distribution within the nucleus and nucleoli of lung cancer cells.<sup>20a,b</sup> Herein, we report the design and use of the new click-capable Pt(II)–azide complex 1 and its cellular distribution in HeLa cells, as observed via confocal fluorescence microscopy. The *in-cell* and *in vitro* reactivity of 1 is also compared with that of the previously reported alkyne-modified congener 2,<sup>26</sup> demonstrating the utility of the completely complementary pair of Pt–click reagents and rhodamine–fluorophore probes. Both compounds 1 and 2 were designed to mimic the *cis* geometry and difunctional reactivity of cisplatin and other Pt(II)-based FDA-approved chemotherapeutics.

## RESULTS AND DISCUSSION

Compound 1 was synthesized analogously to the preparation of 2, with the peptide linkage allowing for facile incorporation of different coupling partners (Figure 2). Therefore, di-*tert*-butyl

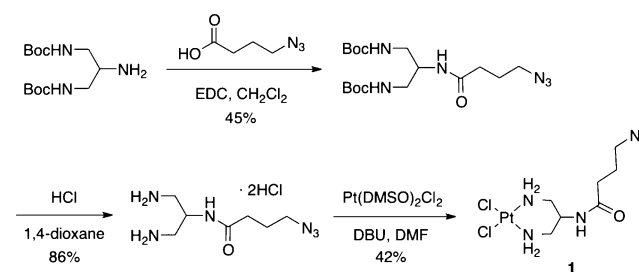


**Figure 2.** Synthesis of Pt complex 1. Boc = *tert*-butoxycarbonyl, EDC = 1-ethyl-3-(3-*N,N*-dimethylaminopropyl)carbodiimide, DMSO = dimethyl sulfoxide, DBU = 1,8-diazabicyclo[5.4.0]undec-7-ene, DMF = *N,N*-dimethylformamide.

(2-aminopropane-1,3-diyl)dicarbamate was coupled to 4-azido-butanoic acid with 1-ethyl-3-(3-*N,N*-dimethylaminopropyl)-carbodiimide.<sup>28</sup> Deprotection with anhydrous HCl followed by platinumation of [Pt(DMSO)<sub>2</sub>Cl<sub>2</sub>] yielded the final product 1 in 16% overall yield. Both complexes 1 and 2 exhibit identical <sup>195</sup>Pt NMR chemical shifts ( $\delta = -2286$  ppm, d<sub>7</sub>-DMF; see Supporting Information), indicating no inter- or intramolecular interactions between the Pt center and peptide-linked azide or alkyne groups.<sup>29</sup>

Crystals of 1 suitable for X-ray diffraction were obtained from a chilled DMF/H<sub>2</sub>O solution, and the structure obtained confirms that assigned via NMR spectroscopy. The individual bond lengths and angles around the square planar Pt(II) center of the azide-containing 1 are very similar to those of the reported alkyne-terminated 2 (see Supporting Information).<sup>26,30</sup> Both compounds form Pt–Pt dimers (Pt⋯Pt, 3.46 Å in 1) connected in the crystal structure by hydrogen bonds (Figure 3 and Supporting Information).<sup>31,32</sup> Each chloride acts as a hydrogen bond acceptor for the Pt-coordinated amine groups (Cl⋯N, 2.53 Å, 2.35 Å in 1) (Figure 3a).<sup>32</sup> In addition, a distance of 2.13 Å between coordinated amine protons and adjacent carbonyl oxygen indicates hydrogen bonding (see Supporting Information, Figure S3).

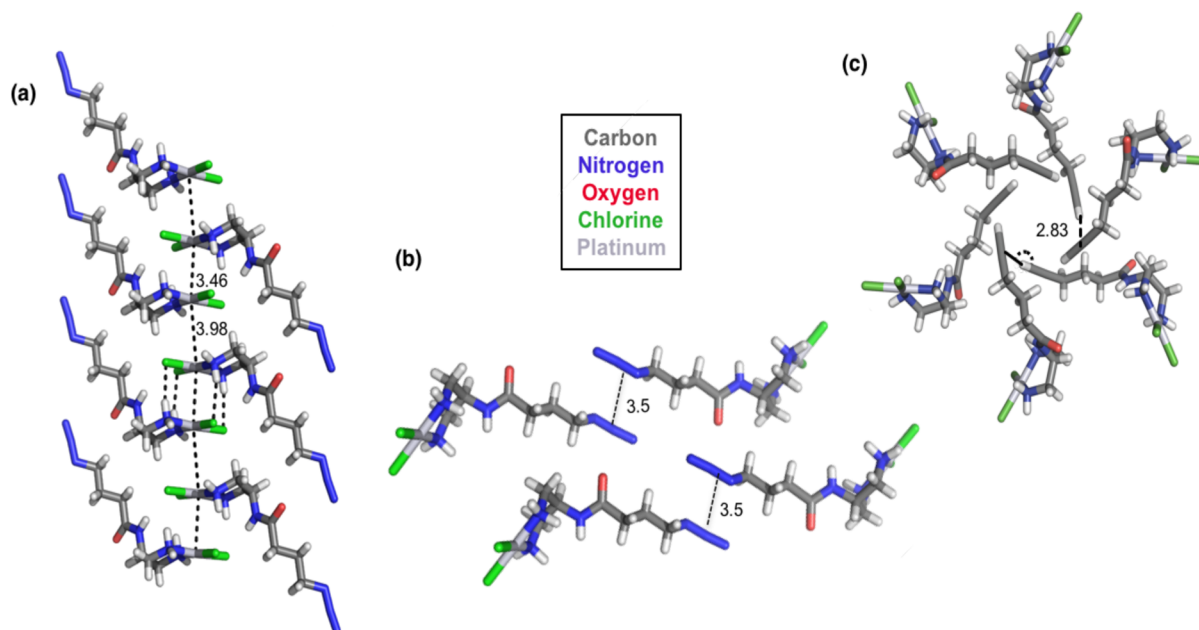


**Figure 3.** (a) Crystal structure arrangement of **1** showing the Pt–Pt dimer formation in a 1D-zigzag chain with a  $159.6^\circ$  angle between the platinum centers as well as Cl...H–N hydrogen bonding. Selected bond lengths and angles: Pt–Cl 2.315(2) Å, 2.334(3) Å; Pt–N 2.016(8) Å, 2.045(7) Å; N≡N 1.117(11) Å; N–N 1.280(12) Å; N≡N–N  $174.2(11)^\circ$ . (b) Antiparallel arrangement of the azide moieties of adjacent Pt chains. (c) Crystal structure arrangement of **2** showing the spoke-type arrangement dictated by CH/ $\pi$ (C≡C) hydrogen bonds. See [Supporting Information](#) for detailed crystallographic data.

Despite the similarities in the solid state between **1** and **2**, the broader packing arrangement changes drastically upon exchange of the alkyne with the azide moiety. The arrangement of **2** is primarily dictated by CH/ $\pi$ (C≡C) hydrogen bonds, forming a rare, spoke-type arrangement (Figure 3c).<sup>26</sup> Arrangement of the azide-containing **1** appears to be dictated by the formation of the Pt dimer, including both Pt–Pt bonding and hydrogen bonds. The Pt centers are aligned into infinite 1D-zigzag chains with regular alternating distances of 3.46 and 3.98 Å and a Pt...Pt...Pt bond angle of  $159.6^\circ$ . Interestingly, the azide moieties of adjacent Pt “chains” are aligned antiparallel and in close proximity to one another, approximately 3.5 Å apart (Figure 3b). This is in agreement with azide–azide packing distances previously reported for several organo-azides and may indicate the presence of a weak dipole–dipole interaction between nitrogen atoms of opposing azides.<sup>33</sup> Finally, N–N bond lengths and angles of the azide moieties themselves are in good agreement with well-established parameters (1.12 and 1.28 Å for the terminal and internal N–N bond distances, respectively, and N≡N–N bond angle of  $174.1^\circ$ ).<sup>33,34</sup>

To confirm the ability of **1** to bind known targets of Pt and subsequently undergo post-binding click modifications, **1** was bound to a short oligonucleotide sequence containing a 5′-GG-3′ pair and subsequently reacted with an alkyne-functionalized rhodamine fluorophore (**3**) (see [Supporting Information](#)) and subjected to denaturing polyacrylamide gel electrophoresis (dPAGE). Both compounds **1** and **2** undergo facile binding to DNA (18 h,  $37^\circ\text{C}$ ), followed by near-complete conversion to the rhodamine-labeled click product ( $\text{CuSO}_4$ –ascorbate, 18 h, rt), the latter complex **2** having been reacted with the analogous azide-functionalized rhodamine fluorophore (**4**) (Figure 4).<sup>35</sup> Both complexes appear to bind to DNA in similar yields, which suggests the identity of the click “handle” (i.e., azide versus

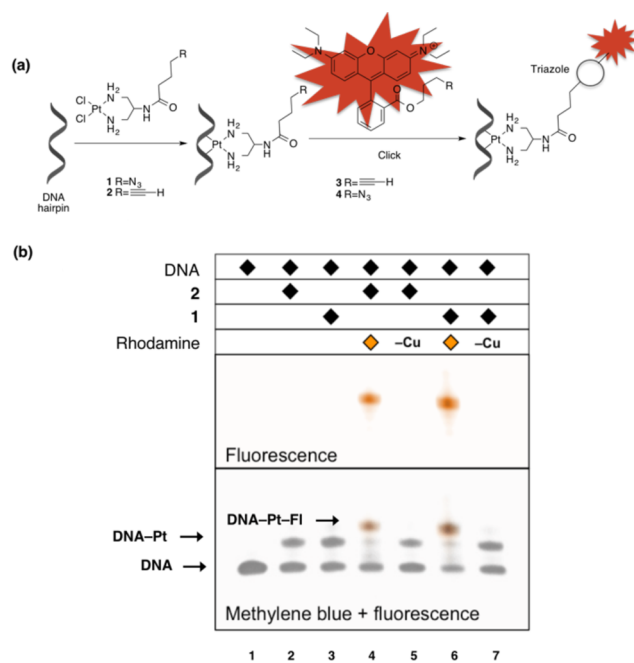


**Figure 4.** (a) Reaction scheme of the binding of **1** and **2** to a DNA hairpin followed by fluorescent click-labeling using complementary alkyne- or azide-rhodamines (**3**, **4**). (b) dPAGE experiment showing the binding of **1** and **2** to a 5′-GG-3′ DNA hairpin (lanes 2 and 3). The click reaction of **1**- and **2**-bound hairpin with the complementary rhodamine fluorophores can be observed by the appearance of a fluorescent band (lanes 4 and 6). Control reactions show no click ligation under Cu-free conditions (lanes 5 and 7).

alkyne) does not significantly affect binding or click reactivity *in vitro*.

Further *in vitro* experiments were conducted to obtain deeper insight into the binding and click reactivity of **1**. Since we now possessed two complementary click-appended Pt(II) complexes, we were curious if they could be reacted together to covalently attach two Pt-bound targets. Solutions of **1** and **2** were individually bound to separate 5'-GG-3' DNA hairpins, then reacted together under click conditions analogous to the previously described reactions with rhodamine (24 h, rt). The appearance of a band of significantly less mobility indicates the formation of the triazole-linked hairpin DNA dimer (lane 4, Figure 5). This result suggests the potential for these Pt compounds to be used in nucleotide cross-linking applications and other diverse nucleotide modification reactions.<sup>36</sup>

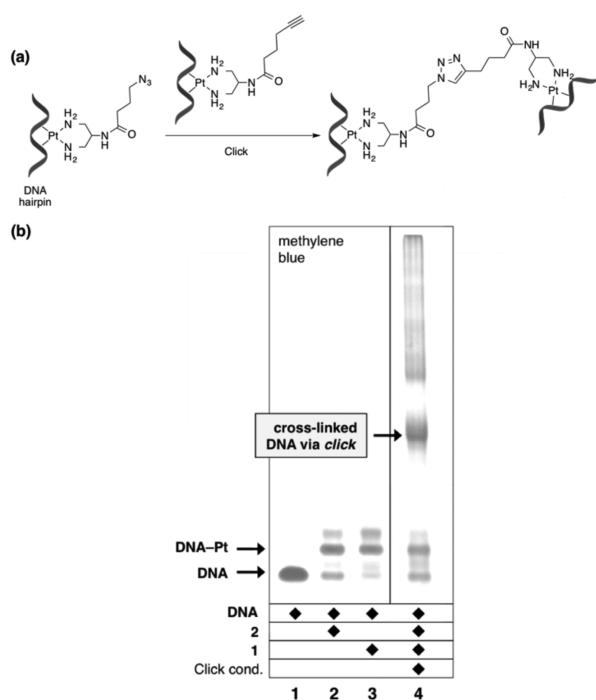


**Figure 5.** (a) Reaction scheme of biomolecule-bound azide **1** clicking to the biomolecule-bound alkyne **2** to form a cross-linked DNA. (b) dPAGE experiment showing **1** and **2** bound to a 5'-GG-3' DNA hairpin (lanes 2 and 3). Lane 4 shows the click reaction product between **1**- and **2**-bound DNA hairpins, resulting in a triazole-linked DNA dimer (see Supporting Information for complete conditions).

To assess the influence of the peptide linkage of **1** (and **2**) on DNA binding and click reactivity, we compared **1** to the peptide- and linker-free *cis*-[Pt(2-azido-1,3-propanediamine)-Cl<sub>2</sub>] (**5**).<sup>37</sup> Compound **5** has been previously utilized by our group for post-treatment fluorescent click labeling of nucleotides and proteins *in vitro*, and rRNA *in vivo*.<sup>25</sup>

For comparison, **1** and **5** were each bound to a 5'-GG-3' DNA hairpin sequence and subjected to click conditions with a dansyl alkyne fluorophore (Figure 6a) and analyzed via dPAGE (Figure 6b). Both compounds appear to bind to DNA in similar yields (lanes 2 and 3), indicating binding reactivity independent of the linker moiety. The click reactivity was evaluated by time-dependent (0.5, 3, or 6 h reaction times) treatment of the Pt–DNA complex with the dansyl–alkyne fluorophore under click conditions. Interestingly, **1**-bound DNA is completely converted to clicked product after only 3 h reaction time, whereas even after 6 h click reaction time, unreacted (non-clicked) **5**-bound DNA is observed (Figure 6,

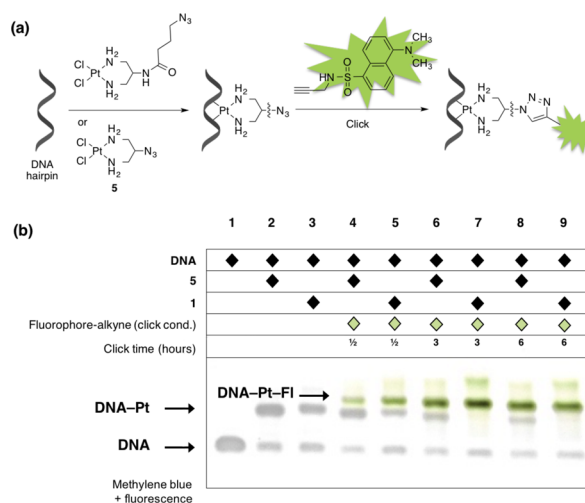


**Figure 6.** (a) Reaction scheme of binding of the azide-modified Pt(II) complexes **1** and **5** to a 5'-GG-3' DNA hairpin sequence, followed by subsequent CuAAC with dansyl alkyne fluorophore. (b) dPAGE analysis of binding and fluorophore conjugation of **1** and **5** to DNA hairpin (see Supporting Information for conditions).

lane 8). The observed enhanced reactivity of the longer **1** may be due to increased steric accessibility of the azide moiety once bound to DNA. Additionally, non-innocence of the peptide bond participating in the click reaction cannot be ruled out—for example, Ting and colleagues reported an acceleration of the CuAAC reaction using organo-azides that contain internal Cu(I) chelating moieties.<sup>38</sup>

Encouraged by its apparent enhanced reactivity, we pursued cellular localization studies using the azide-appended **1** and confocal fluorescence microscopy (Figure 7). In initial studies, HeLa cells were treated with **1** (25 μM, 3 h), washed, fixed and permeabilized, and then labeled with the alkyne-containing rhodamine fluorophore **3** (5 μM, 2 h) under CuAAC click conditions (see Supporting Information). Confocal images of the cells show the highest level of fluorescence in the nucleoli of the HeLa cells, along with broad localization in the nucleus (Figure 7b). Importantly, the Cu-free controls show no fluorescence from nonspecific fluorophore interactions (Figure 7f and Supporting Information). These results are consistent with previously reported targets of Pt(II) chemotherapeutics. The high accumulation of compound **1** in the nucleoli is in agreement with previously identified nuclear DNA adducts of Pt,<sup>10</sup> as well as Pt–rRNA adducts. rRNA has been shown to bind Pt(II) complexes using inductively coupled plasma mass spectrometry and fluorescent labeling in *Saccharomyces cerevisiae*.<sup>24,27</sup> Pt–protein adducts may also be present. The nucleolus has also been identified as a major target using some fluorophore pre-tethered Pt(II) complexes.<sup>39</sup> Bierbach and colleagues very recently identified localization in the nucleolus using an azide-modified Pt–acridine complex for post-binding fluorescent labeling as well as pre-tethered Pt–fluorophores, although differences between the two approaches were noted.<sup>20a,b</sup>

Treatment of HeLa cells using the complementary alkyne-containing complex **2** and the rhodamine-azide **4** (25 μM treatment) shows identical localization (Figure 7d), which indicates similar cellular binding of both Pt complexes **1** and **2** independent of the click-functionalized moiety. Interestingly, however, Pt(II)-concentration-dependent post-treatment labeling in the HeLa cell line shows a dramatic difference in the

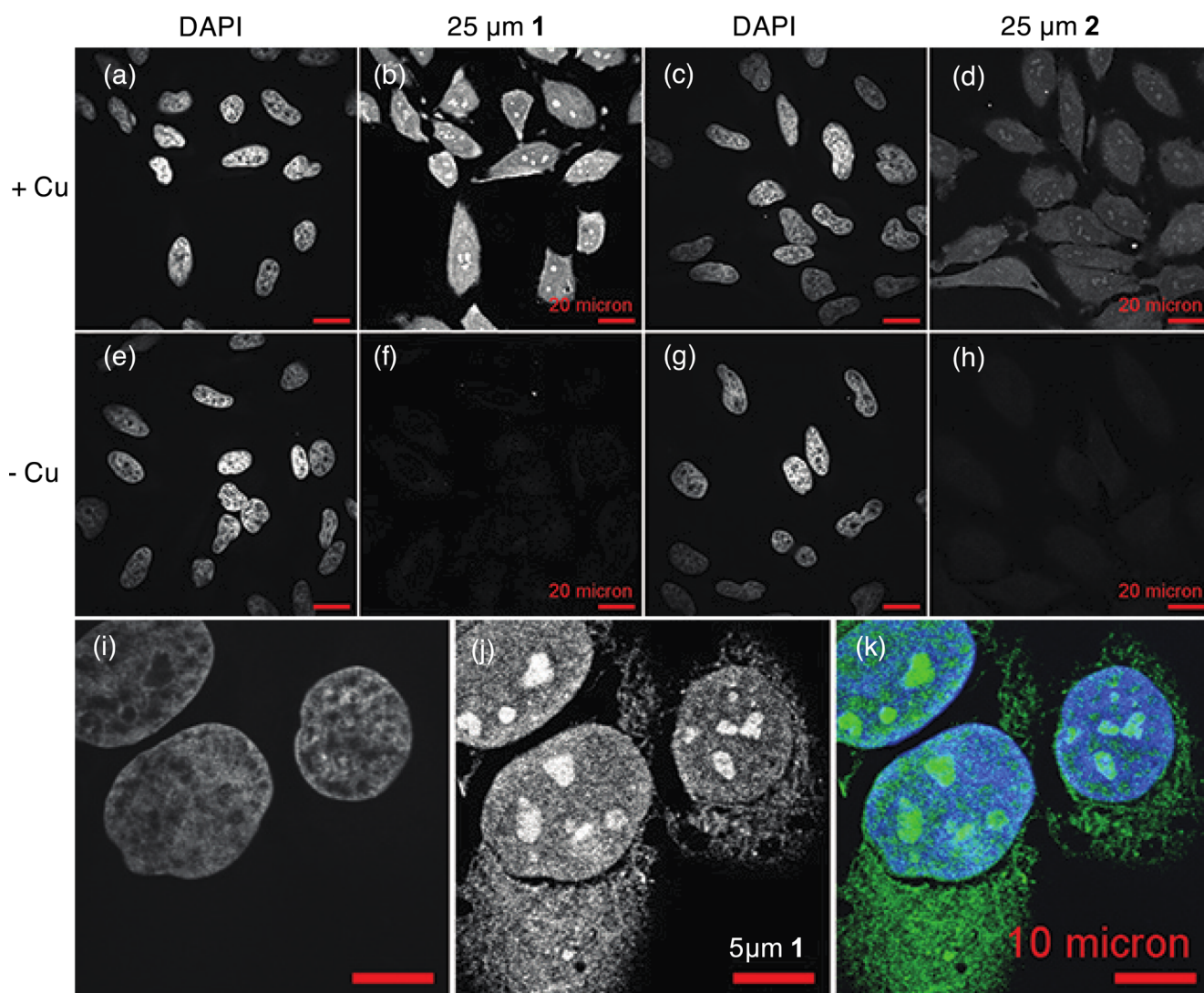


**Figure 7.** Confocal image of fluorescent cellular localization. Panel (b) shows the fluorescent labeling of HeLa cells treated with **1** ( $25\ \mu\text{M}$ , 3 h) and subsequent click with rhodamine alkyne **3**. The Cu-free control (f) shows no fluorescence. Panel (d) shows the fluorescent labeling of HeLa Cells treated with **2** ( $25\ \mu\text{M}$ , 3 h) after fixation, permeabilization, and labeling with the rhodamine azide **4** in the HeLa cell line and Cu-free control (h). Panel (j) shows an enlarged image of the fluorescent labeling of HeLa cells treated with **1** ( $5\ \mu\text{M}$ , 3 h) and subsequent click with rhodamine alkyne **3**. The overlay of the DAPI stain and rhodamine labeling is depicted in (k).

observed fluorescent signal between these two complementary click compounds. Despite the similar localization of **1** and **2**, there is significantly less fluorescent signal following  $25\ \mu\text{M}$  cellular treatment with **2**, using identical conditions. HeLa cells were also treated individually with  $5\ \mu\text{M}$  complex **1** and **2** for 3 h followed by click labeling with the complementary rhodamine fluorophores. At this lower concentration, cells treated with the alkyne-appended complex **2** show no detectable fluorescent signal above background, but cells treated with azide-containing **1** present bright and distinct fluorescence (Figure 7j). Although we have not observed Pt-catalyzed hydration or hydroamination across the triple bond in previous experiments using **2**, it is well-reported that alkyne-containing compounds can undergo these reactions, which could lead to a decrease in fluorescent signal in-cell.<sup>40</sup> The hydrophobicity of alkynes in comparison to their azide counterparts may also have an effect on accumulation or reactivity in the cell. These promising results show the potential of compound **1** not only for further localization studies in different cancer cell lines, but also for

ongoing goals of isolating and identifying Pt(II)-bound targets using click chemistry.

## CONCLUSIONS

In summary, we have developed a novel azide-containing Pt(II) complex (**1**) and compared it to its alkyne-containing congener (**2**), and we report here for the first time the post-treatment fluorescent labeling of a bifunctional cisplatin-based Pt(II) complex in the HeLa cancer cell line. The exchange of the alkyne to the azide moiety leads to a completely different arrangement in the solid state, with the alkyne-containing **2** forming a circular arrangement dominated by CH/ $\pi(\text{C}\equiv\text{C})$  hydrogen bonds and secondary Pt–Pt dimer interactions. In contrast, the arrangement of the azide analogue is dominated by Pt–Pt dimer formation and hydrogen bonding forming a 1D-zigzag chain. In solution both complexes bind similarly to a DNA hairpin and show similar click reactivity in post-binding fluorescent labeling using complementary click-modified rhodamine fluorophores. Not only were we able to show the

utilization of **1** as a cross-linking agent for larger biomolecules, but we also demonstrated its faster click reactivity in comparison to a previously described azide-containing Pt(II) complex. Finally, we report the first post-treatment fluorescent labeling of a cisplatin-like bifunctional Pt(II) complex in HeLa cells, observing Pt(II) localization in the nuclei and distinctively in the nucleoli. Concentration-dependent localization showed stronger fluorescent signals using the azide **1** versus the alkyne **2** Pt complex. These results show the potential of the novel compound **1** for further cell-line-dependent localization studies and the isolation of Pt(II)-bound targets.

## ■ ASSOCIATED CONTENT

### Supporting Information

The Supporting Information is available free of charge on the ACS Publications website at DOI: 10.1021/jacs.5b09108.

Text and figures giving methods, experimental procedures, syntheses, dPAGE data, confocal microscopy data, and NMR spectra (PDF)

X-ray crystallographic data for **1** (CIF)

## ■ AUTHOR INFORMATION

### Corresponding Author

\*derose@uoregon.edu

### Author Contributions

R.W., J.D.W., and A.D.M. contributed equally to this work.

### Notes

The authors declare no competing financial interest.

## ■ ACKNOWLEDGMENTS

The authors thank the National Science Foundation (CHE-1413677 to V.J.D.) for funding.

## ■ REFERENCES

- (1) Rozenzweig, M.; Von Hoff, D. D.; Slavik, M.; Muggia, F. M. *Ann. Int. Med.* **1977**, *86*, 803.
- (2) Harper, B. W.; Krause-Heuer, A. M.; Grant, M. P.; Manohar, M.; Garbutcheon-Singh, K. B.; Aldrich-Wright, J. R. *Chem. - Eur. J.* **2010**, *16*, 7064.
- (3) Dyson, P. J.; Sava, G. *Dalton Trans.* **2006**, 1929.
- (4) Rosenberg, B.; Renshaw, E.; Van Camp, L.; Hartwick, J.; Drobnik, J. *J. Bacteriol.* **1967**, *93*, 716.
- (5) Sava, G.; Jaouen, G.; Hillard, E. A.; Bergamo, A. *Dalton Trans.* **2012**, *41*, 8226.
- (6) Casini, A.; Reedijk, J. *Chem. Sci.* **2012**, *3*, 3135.
- (7) Guggenheim, E. R.; Xu, D.; Zhang, C. X.; Chang, P. V.; Lippard, S. J. *ChemBioChem* **2009**, *10*, 141.
- (8) Wexselblatt, E.; Yavin, E.; Gibson, D. *Inorg. Chim. Acta* **2012**, *393*, 75.
- (9) Arnesano, F.; Losacco, M.; Natile, G. *Eur. J. Inorg. Chem.* **2013**, 2701.
- (10) Wang, D.; Lippard, S. J. *Nat. Rev. Drug Discovery* **2005**, *4*, 307.
- (11) Jamieson, E. R.; Lippard, S. J. *Chem. Rev.* **1999**, *99*, 2467.
- (12) Todd, R. C.; Lippard, S. J. *Metalomics* **2009**, *1*, 280.
- (13) (a) Caradonna, J. P.; Lippard, S. J.; Gait, M. J.; Singh, M. J. *Am. Chem. Soc.* **1982**, *104*, 5793. (b) Fichtinger-Schepman, A. M. J.; Van der Veer, J. L.; Den Hartog, J. H. J.; Lohman, P. H. M.; Reedijk, J. *Biochemistry* **1985**, *24*, 707. (c) Eastman, A. *Biochemistry* **1986**, *25*, 3912. (d) Terheggen, P. M. A. B.; Floot, B. G. J.; Scherer, E.; Begg, A. C.; Fichtinger-Schepman, A. M. J.; Den Engelse, L. *Cancer Res.* **1987**, *47*, 6719.
- (14) (a) DeConti, R. C.; Toftness, B. R.; Lange, R. C.; Creasey, W. A. *Cancer Res.* **1973**, *33*, 1310. (b) Akaboshi, M.; Kawai, K.; Ujeno, Y.; Takada, S.; Miyahara, T. *Jpn. J. Cancer Res.* **1994**, *85*, 106. (c) Akaboshi,

M.; Kawai, K.; Maki, H.; Akuta, K.; Ujeno, Y.; Miyahara, T. *Jpn. J. Cancer Res.* **1992**, *83*, 522.

(15) (a) Wisnovsky, S. P.; Wilson, J. J.; Radford, R. J.; Pereira, M. P.; Chan, M. R.; Laposa, R. R.; Lippard, S. J.; Kelley, S. O. *Chem. Biol.* **2013**, *20*, 1323. (b) Yu, F.; Megyesi, J.; Price, P. M. *Am. J. Physiol. Renal Physiol.* **2008**, *295*, F44.

(16) *Inter alia* (a) Gemba, M.; Nakatani, E.; Teramoto, M.; Nakano, S. *Toxicol. Lett.* **1987**, *38*, 291. (b) Samimi, G.; Katano, K.; Holzer, A. K.; Safaei, R.; Howell, S. B. *Mol. Pharmacol.* **2004**, *66*, 25. (c) Samimi, G.; Safaei, R.; Katano, K.; Holzer, A. K.; Rochdi, M.; Tomioka, M.; Goodman, M.; Howell, S. B. *Clin. Cancer Res.* **2004**, *10*, 4661. (d) Jansen, B. A. J.; Wielaard, P.; Kalayda, G. V.; Ferrari, M.; Molenaar, C.; Tanke, H. J.; Brouwer, J.; Reedijk, J. *JBIC, J. Biol. Inorg. Chem.* **2004**, *9*, 403. (e) Chapman, E. G.; Hostetter, A.; Osborn, M.; Miller, A.; DeRose, V. J. In *Metal Ions In Life Sciences: Structural and Catalytic Roles of Metal Ions in RNA*; Sigel, A., Sigel, H., Sigel, R. K. O., Eds.; Royal Society of Chemistry: Cambridge, U.K., 2011. (f) Kalayda, G. V.; Jansen, B. A. J.; Molenaar, C.; Wielaard, P.; Tanke, H. J.; Reedijk, J. *JBIC, J. Biol. Inorg. Chem.* **2004**, *9*, 414. (g) Kalayda, G. V.; Jansen, B. A. J.; Wielaard, P.; Tanke, H. J.; Reedijk, J. *JBIC, J. Biol. Inorg. Chem.* **2005**, *10*, 305. (h) Beretta, G. L.; Righetti, S. C.; Lombardi, L.; Zunino, F.; Perego, P. *Ultrastruct. Pathol.* **2002**, *26*, 331. (i) Meijer, C.; Van Luyn, M. J. A.; Nienhuis, E. F.; Blom, N.; Mulder, N. H.; De Vries, E. G. E. *Biochem. Pharmacol.* **2001**, *61*, 573. (j) Khan, M. U. A.; Sadler, P. J. *Chem.-Biol. Interact.* **1978**, *21*, 227. (k) Berry, J. P.; Galle, P.; Viron, A.; Kacerovská, H.; Macieira-Coelho, A. *Biomed. Pharmacother.* **1983**, *37*, 125. (l) Hall, M. D.; Hambley, T. W.; Beale, P.; Zhang, M.; Dillon, C. T.; Foran, G. J.; Stampfl, A. P.; Lai, B. J. *Inorg. Biochem.* **2003**, *96*, 141. (m) Hall, M. D.; Alderden, R. A.; Zhang, M.; Beale, P. J.; Cai, Z.; Lai, B.; Stampfl, A. P.; Hambley, T. W. *J. Struct. Biol.* **2006**, *155*, 38.

(17) Molenaar, C.; Teuben, J.-M.; Heetebrij, R. J.; Tanke, H. J.; Reedijk, J. *JBIC, J. Biol. Inorg. Chem.* **2000**, *5*, 655.

(18) Safaei, R.; Katano, K.; Larson, B. J.; Samimi, G.; Holzer, A. K.; Naerdemann, W.; Tomioka, M.; Goodman, M.; Howell, S. B. *Clin. Cancer Res.* **2005**, *11*, 756.

(19) White, J. D.; Haley, M. M.; DeRose, V. J. *Acc. Chem. Res.* **2015**, in press.

(20) (a) Ding, S.; Qiao, X.; Suryadi, J.; Marrs, G. S.; Kucera, G. L.; Bierbach, U. *Angew. Chem., Int. Ed.* **2013**, *52*, 3350. (b) Qiao, X.; Ding, S.; Liu, F.; Kucera, G. L.; Bierbach, U. *JBIC, J. Biol. Inorg. Chem.* **2014**, *19*, 415. (c) Wexselblatt, E.; Yavin, E.; Gibson, D. *Inorg. Chim. Acta* **2012**, *393*, 75. (d) Ghosh, B.; Jones, L. H. *MedChemComm* **2014**, *5*, 247.

(21) Rijal, K.; Bao, X.; Chow, C. S. *Chem. Commun.* **2014**, *50*, 3918.

(22) Kolb, H. C.; Finn, M. G.; Sharpless, K. B. *Angew. Chem., Int. Ed.* **2001**, *40*, 2004.

(23) White, J. D.; Osborn, M. F.; Moghaddam, A. D.; Guzman, L. E.; Haley, M. M.; DeRose, V. J. *J. Am. Chem. Soc.* **2013**, *135*, 11680.

(24) Osborn, M. F.; White, J. D.; Haley, M. M.; DeRose, V. J. *ACS Chem. Biol.* **2014**, *9*, 2404.

(25) Moghaddam, A. D.; White, J. D.; Cunningham, R. M.; Loes, A. N.; Haley, M. M.; DeRose, V. J. *Dalton Trans.* **2015**, *44*, 3536.

(26) White, J. D.; Guzman, L. E.; Zakharov, L. N.; Haley, M. M.; DeRose, V. J. *Angew. Chem., Int. Ed.* **2015**, *54*, 1032.

(27) Hostetter, A. A.; Osborn, M. F.; DeRose, V. J. *ACS Chem. Biol.* **2012**, *7*, 218.

(28) Ramalingam, K.; Raju, N.; Nanjappan, P.; Nowotnik, D. P. *Tetrahedron* **1995**, *51*, 2875.

(29) Still, B. M.; Kumar, P. G. A.; Aldrich-Wright, J. R.; Price, W. S. *Chem. Soc. Rev.* **2007**, *36*, 665.

(30) X-ray data for **1**: C<sub>7</sub>H<sub>16</sub>Cl<sub>2</sub>N<sub>6</sub>O<sub>4</sub>Pt, *M* = 466.25, 0.07 × 0.04 × 0.03 mm, *T* = 173 K, triclinic, space group  $P\bar{1}$ , *a* = 7.330(2) Å, *b* = 7.583(2) Å, *c* = 11.831(3) Å,  $\alpha$  = 85.465(5)°,  $\beta$  = 86.040(5)°,  $\gamma$  = 86.498(5)°, *V* = 653.1(3) Å<sup>3</sup>, *Z* = 2, *D<sub>c</sub>* = 2.371 Mg/m<sup>3</sup>,  $\mu$ (Mo) = 11.147 mm<sup>-1</sup>, *F*(000) = 440, 2 $\theta$ <sub>max</sub> = 50.0°, 7931 reflections, 2287 independent reflections [*R*<sub>int</sub> = 0.0774], *R*1 = 0.0403, *wR*2 = 0.0644, and *GOF* = 1.011 for 2287 reflections (154 parameters) with *I* > 2 $\sigma$ (*I*), *R*1 = 0.0627, *wR*2 = 0.0704, and *GOF* = 1.011 for all reflections, max/min residual electron density +1.423/−1.283 e/Å<sup>3</sup>.

- (31) Woollins, J. D.; Kelly, P. F. *Coord. Chem. Rev.* **1985**, *65*, 115.
- (32) Odoko, M.; Okabe, N. *Acta Crystallogr., Sect. C: Cryst. Struct. Commun.* **2006**, *62*, m136.
- (33) (a) Guo, L.; Thompson, C. M.; Twamley, B. *Acta Crystallogr., Sect. C: Cryst. Struct. Commun.* **2009**, *65*, o179. (b) Yang, H.; Carter, R. G. *J. Org. Chem.* **2010**, *75*, 4929. (c) Brady, R. M.; Zhang, M.; Gable, R.; Norton, R. S.; Baell, J. B. *Bioorg. Med. Chem. Lett.* **2013**, *23*, 4892. (d) Parsons, S.; Haxton, A.; Flitsch, S.; Wood, P. A., private communication to the Cambridge Crystallographic Data Centre, 2004; DOI:10.5517/cc88jrs.
- (34) (a) Bräse, S.; Gil, C.; Knepper, K.; Zimmermann, V. *Angew. Chem., Int. Ed.* **2005**, *44*, 5188. (b) Chen, F.-F.; Wang, F. *Molecules* **2009**, *14*, 2656.
- (35) Baier, G.; Siebert, J. M.; Landfester, K.; Musyanovych, A. *Macromolecules* **2012**, *45*, 3419.
- (36) Chapman, E. G.; DeRose, V. J. *J. Am. Chem. Soc.* **2012**, *134*, 256.
- (37) Urankar, D.; Košmrlj, J. *Inorg. Chim. Acta* **2010**, *363*, 3817.
- (38) Uttamapinant, C.; Tangpeerachaikul, A.; Grecian, S.; Clarke, S.; Singh, U.; Slade, P.; Gee, K. R.; Ting, A. Y. *Angew. Chem., Int. Ed.* **2012**, *51*, 5852.
- (39) (a) Liang, X.-J.; Shen, D.-W.; Chen, K. G.; Wincovitch, S. M.; Garfield, S. H.; Gottesman, M. M. *J. Cell. Physiol.* **2005**, *202*, 635. (b) Colombo, A.; Fiorini, F.; Septiadi, D.; Dragonetti, C.; Nisic, F.; Valore, A.; Roberto, D.; Mauro, M.; De Cola, L. *Dalton Trans.* **2015**, *44*, 8478. (c) Shen, C.; Harris, B. D. W.; Dawson, L. J.; Charles, K. A.; Hambley, T. W.; New, E. J. *Chem. Commun.* **2015**, *51*, 6312. (d) Wu, S.; Zhu, C.; Zhang, C.; Yu, Z.; He, W.; He, Y.; Li, Y.; Wang, J.; Guo, Z. *Inorg. Chem.* **2011**, *50*, 11847.
- (40) Belluco, U.; Bertani, R.; Michelin, R. A.; Mozzon, M. *J. Organomet. Chem.* **2000**, *600*, 37.